ELSEVIER

Biophysical Chemistry 78 (1999) 247–257

Biophysical Chemistry

Long-term molecular dynamics simulation of copper azurin: structure, dynamics and functionality

Caterina Arcangeli[a,b], Anna Rita Bizzarri[a,b], Salvatore Cannistraro[a,b,*]

[a] *Unita' INFM, Dipartimento di Fisica dell'Universita', I-06100 Perugia, Italy*
[b] *Dipartimento di Scienze Ambientali, Universita' della Tuscia, I-01100 Viterbo, Italy*

Received 12 November 1998; received in revised form 18 February 1999; accepted 18 February 1999

Abstract

A long-term molecular dynamics simulation (1.1 ns), at 300 K, of fully hydrated azurin has been performed to put into relationship the protein dynamics to functional properties with particular attention to those structural elements involved in the electron transfer process. A detailed analysis of the root mean square deviations and fluctuations and of the intraprotein H-bonding pattern has allowed us to demonstrate that a rigid arrangement of the β-stranded protein skeleton is maintained during the simulation run, while a large mobility is registered in the solvent-exposed connecting regions (turns) and in the α-helix. Moreover, the structural elements, likely involved in the electron transfer path, show a stable H-bonding arrangement and low fluctuations. Analysis of the dynamical cross-correlation map has revealed the existence of correlated motions among residues connected by hydrogen bonds and of correlated and anti-correlated motions between regions which are supposed to be involved in the functional process, namely the hydrophobic patch and the regions close to the copper reaction center. The results are briefly discussed also in connection to the current through-bond tunneling model for the electron transfer process. Finally, a comparison with the structural and the dynamical behaviour of plastocyanin, whose structure and functional role are very similar to those of azurin, has been performed.

Keywords: Azurin; Electron transfer; Molecular dynamics

* Corresponding author. Fax: +39-075-44666, e-mail:cannistraro@pg.infn.it

0301-4622/99/$ - see front matter
PII: S0301-4622(99)00029-0

1. Introduction

The wide variety of different functions performed by proteins is in intimate relationship to the large variability which characterizes the structural organization of these biomolecules. Actually, the spatial arrangement of protein atoms directly reflects the specific biological role played by the macromolecule; e.g. the flexibility of large portions of the protein molecule, as well as the conformational changes involved in the functional role, are strongly-dependent on the particular secondary structure in which the macromolecule is arranged. In this respect, it is generally assumed that the intraprotein H-bonds play a crucial role to determine and stabilize the secondary and tertiary structure, as stressed by studies of protein structure mutations [1].

At the same time, protein dynamics is closely related to the structural features of the macromolecule. Large amplitude motions, possibly responsible for the transitions among conformational substates, the sampling of which is relevant for the biological functionality [2], require strongly correlated displacements of large parts of the macromolecule; such a behaviour revealing a marked dependence on the protein architecture and on the solvent composition [3]. On the other hand, fast local motions (librations and vibrations of atoms or groups of atoms) show a sort of universal character whose features can be strongly modulated by the surrounding solvent. In this respect, it is interesting to note that the solvent-exposed side-chains reveal relaxations closely reminiscent of fast (or β) relaxations observed in glassy materials and they could be the precursor of the slower (or α) relaxations involving main-chain collective motions [4].

Generally, to completely elucidate the functional role of a protein, a full understanding of its structure and dynamics, and of their relationship, is required. Molecular dynamics (MD) simulation, which allows one to investigate the temporal and structural fluctuations of both the protein and the surrounding solvent at atomic resolution, has become a rewarding tool to get some new insights into the relationship between the structure, the dynamics and the functionality of a protein. MD approach covers, up to day, the time scale from fs up to some ns, and is warranted by the fact that the force fields employed are able to well reproduce the spectroscopic experiments performed on the same time scale. Recently, we have been strongly interested in the application of the MD simulation approach to the study of the behaviour at the protein–water interface in a small copper protein, plastocyanin (PC) [5–9], and also to the investigation of the dynamical behaviour of PC in relationship to its functional role [10], which consists mainly in acting as an electron transfer agent in the photosynthetic system [11]. More recently, we have also focused our attention on the comparison of the MD simulation results with those obtained from neutron scattering experiments on the blue copper protein, azurin (AZ) [12], whose β-sandwich secondary structure, electron transfer function and spectroscopic features are very similar to those of PC. The experimental dynamical structure factor of AZ has shown the presence of an excess of vibrational modes situated at approximately 3 meV [12,13]; such an inelastic peak being reminiscent of the so-called boson peak, frequently encountered in a glassy system [14]. The presence of such a peak was confirmed by MD simulations of AZ [12,13], and strikingly enough a similar excess of mode was demonstrated also in hydrated water of PC [15] and of AZ [16]. In this respect, we have speculated about the possible role played by this excess of modes in the dynamical coupling between the protein and the hydrated water [12,13,15,16].

On such a ground, a deeper characterization, at atomic resolution, of the dynamical behaviour of the fully hydrated AZ is required. In the present paper, with the help of MD simulation, we have tried to better elucidate the structure and the dynamics of AZ by also paying attention to those structural aspects related to the electron transfer process, namely the hydrophobic patch, which is involved in the electron transfer reaction with its physiological redox partners [17,18], and the possible through-bond electron transfer routes [19–21]. To this aim, we have analyzed in detail a number of dynamical properties of AZ, such as the root mean square deviations and fluctuations, the intraprotein H-bonding pattern and the dy-

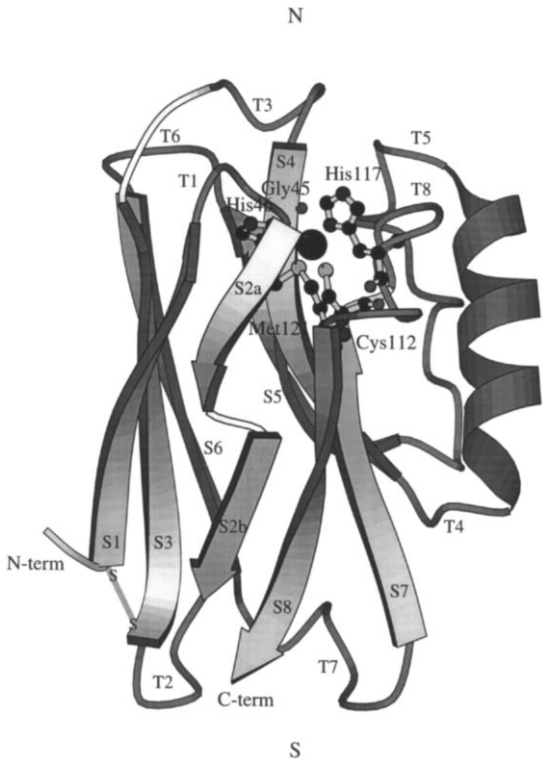

Fig. 1. Model of AZ crystallographic structure, showing 8 β-strands (S), 8 turn regions (T) and the α-helix. The copper atom (dark sphere) is shown at the top, surrounded by the five ligands (ball and stick). The disulphide bridge (-S–S-), which is supposed to be involved in the electron tranfer mechanism, is also shown. The northern (N) and southern (S) end of the protein to which we refer in the text, are indicated. This drawing was generated with crystallographic coordinates from ref. [22] and using the program Molscript [38].

namical cross-correlation map. In addition, a comparison with the results obtained for PC has been performed to demonstrate the emerging similarities and differences between the two proteins.

2. Computational methods

AZ (128 amino acids, 14 kDa) consists of eight stranded β-strands, arranged in a β-sandwich, connected by random chains (turns) and of an α helical insertion (see Fig. 1). The copper site is at the top, or northern end, of protein, surrounded by an extensive hydrophobic patch that is the most striking surface feature of the protein [17,18].

Initial coordinates of AZ are from the X-ray crystal structure of *Pseudomonas aeruginosa* oxidized (Cu^{2+}) AZ at 0.193 nm resolution (4AZU entry of Brookhaven Protein Data Bank) [22]. In particular, the entry coordinates have been derived from the second segment (denoted by B) of the tetramer composing the crystal unit. The MD trajectories of AZ have been generated by an integration step of 0.002 ps, using the GROMOS87 program package [23] with the force field modified according to ref [24].

The disulphide bridge between the 3 and 26 residues, joining the ends of the S1 and S3 β-strands, has been introduced. The copper, located approximately 7Å below the protein surface, is coordinated to two side chain nitrogens (His46 and His117) and to two side chain sulfurs (Cys112 and Met121); the latter one being weaker than the former one. The resulting geometric and the electronic structure of the copper site are closely reminiscent of that of PC. However, nuclear magnetic resonance experiments [25] have demonstrated the presence of a weak fifth ligand (a carbonyl oxygen from Gly45) which determines a distorted trigonal bipyramidal geometry to the copper site. Since the GROMOS force field does not include parameters for amino acids liganded to metal ions, a modified force field has been employed. According to the recent approach used for PC, a covalent bond between the copper and each ligand has been introduced to preserve the X-ray structure [10]. This choice, supported, on the other hand, by spectroscopic evidence of a general covalent nature for the copper-binding site [11], resulting in a more realistic picture than that obtained with the electrostatic method previously used [5,6]. A similar approach has also been used to treat the copper site of PC in a MD simulation work focused on the photo-induced electron transfer dynamics [26].

All the ionizable residues, with the exception of copper ligands, have been assumed to be in the ionization state corresponding to pH 5.5 of the crystal. The charge of Cys112 has been set to -0.5e, while His46, His117, Met121 and Gly45

have been considered neutral; a charge of 0.5e has been assigned to the copper ion. The resulting total protein charge is then −3.0e. The protein molecule has been centered in a truncated octahedron obtained from a cube of edge 6.34998 nm filled with bulk SPC/E waters [27]. A minimum distance of 0.785 nm between the solute atoms and the box edges has been maintained. Any water molecule placed to a distance from any protein atom smaller than 0.23 nm has been removed to give a final fully hydrated system containing 3662 water molecules corresponding to 4.7 g of water per g of protein. To avoid edge effects and to better describe the condition of full hydration, periodic boundary conditions have been applied. Cut-off radii of 0.8 nm for the non-bonded interactions and of 1.4 nm for the long-range charged interactions have been used. During 200 steps of energy minimization with the steepest descent method, a harmonic position restraining force with a constant equal to 9000 KJ mol^{-1} nm^{-2} has been used to minimize deviations from the X-ray structure. Longer energy minimizations, using also the conjugate gradient method, have been performed without a real improvement of the minimized structure. Initial atomic velocities have been assigned from a Maxwellian distribution corresponding to 250 K [28]. Any residual translational and rotational motion of the center of mass has been removed from the initial velocities. The temperature has been kept fixed at 250 K for the first 6 ps, then it has been increased by 5 K every 4 ps to reach the value of 300 K which has been maintained throughout the following simulation. The temperatures of the protein and the solvent have been separately coupled to an external bath with relaxation times of 0.1 ps. A decreasing positional restraining force, with a constant going from 9000 KJ mol^{-1} nm^{-2} to 50 KJ mol^{-1} nm^{-2} also has been applied during the first 40 ps.

The MD simulation consisted of a total run of 1100 ps. Configurations of all trajectories and energy have been saved every 0.1 ps. The neighbour pair list has been updated every 10 steps. The Shake constraint algorithm [29] has been used throughout the simulation to fix the internal geometry of water molecules and to keep bond lengths of protein rigorously fixed at their equilibrium values.

The dynamical properties of AZ, discussed below, have been computed by averaging on the 300–1100 ps time window and after having removed the overall translational and rotational protein diffusions by superimposing the backbone of each configuration onto the backbone of the starting AZ structure using a mass-weighted least-squares fitting algorithm [30].

The mass-weighted radius of gyration (R_g) of the AZ has been obtained from:

$$R_g = \left[\left(\frac{\Sigma_i m_i r_i^2}{\Sigma_i m_i} \right) \right]^{1/2} \quad (1)$$

where r_i is the distance between atom i and the center of mass of the protein and m_i is the mass of atom i.

The root mean square deviations (RMSD) and fluctuations (RMSF) of atomic positions in the simulation run have been calculated according to:

$$\Delta R = \left[\frac{1}{N_{at}} \sum_{i=1}^{N_{at}} \langle \{ (\Delta x_i)^2 + (\Delta y_i)^2 + (\Delta z_i)^2 \} \rangle \right]^{1/2} \quad (2)$$

where N_{at} is the total number of atoms and the brackets $\langle \cdots \rangle$ represent a time average. In computing the RMSD, Δx_i, Δy_i and Δz_i are the differences between the instantaneous and the starting atomic coordinates for the ith atom, while in computing the RMSF, they are the differences between the instantaneous and the averaged atomic coordinates for the ith atom. The positional RMSF derived from crystallographic B-factors have been calculated according to the expression:

$$\Delta R = \left(\frac{3B_i}{8\pi^2} \right)^{1/2} \quad (3)$$

The dynamical cross-correlation map (DCCM) is a matrix representation of the time-correlated information between protein atoms i and j (C_{ij}),

and has been calculated using the following equation [31]:

$$C_{ij} = \frac{\langle r_i r_j \rangle - \langle r_i \rangle - \langle r_j \rangle}{\left[\left(\langle r_i^2 \rangle - \langle r_i \rangle^2\right)\left(\langle r_j^2 \rangle - \langle r_j \rangle^2\right)\right]^{1/2}} \quad (4)$$

Therefore, DCCM provides the correlation coefficients for residue displacements along a straight line: positive values are indicative of motions in the same direction, while negative values are indicative of motions in the opposite direction.

3. Results and discussion

To assess the stability of the simulation and to check that the protein has properly equilibrated, a collection of dynamical properties as a function of the simulation time was monitored and is reported in Table 1. The radius of gyration, R_g, of the protein fluctuates around a mean value of 1.355 nm, which is consistent with that expected for the hydrated protein. Its analysis as a function of simulation time shows an initial slow decrease up to the first 300 ps, after that fluctuations around a stable value occur (data not shown). The time evolution of the potential and kinetic total energies, whose mean values are reported in Table 1, reveals that, after a transient period of approximately 45 ps, both the energies are almost stable (data not shown). Concerning the overall RMSD from the crystal structures, which are found to be higher for the all protein atoms than for the C_α protein atoms, they are in agreement with other protein simulations and indicate a substantially slight displacement from the crystal structure during all the simulation run.

The RMSD of all AZ atoms as a function of simulation time are plotted in the inset of Fig. 2. An initial rise is followed by small fluctuations between 0.15 and 0.18 nm, indicating that protein structure is practically stable after 300 ps.

The time-averaged (over 700 ps) RMSD from the atom positions in the AZ crystal, as a function of the backbone atoms (N, C_α, C, and O), are shown in Fig. 2. We observe the largest RMSD values (more than 0.4 nm) which correspond to the 72–78 residues belonging to the T5 turn which connects the sheet core with the α helix, and of the 3–5 residues, close to the N-term of the protein involved in the initial part of the S1 β-strand. Minor peaks (approx. 0.25 nm) are registered for the 34–40 residues and the 50–57 residues belonging to the terminal part of the S3, and S4 β-strands, respectively. In addition, another peak is registered approximately 99–110 residues which are located at the T7 turn connecting the S6 and the S7 β-strands.

Generally, the RMSD provide information about the conformational changes occurring during the simulation, with respect to the initial crystallographic structure. The results indicate that the largest changes take place whitin the residues located on the external surface; this behaviour is similar to that observed for PC [10], and is indicative of the action of hydration water upon the solvent exposed backbone atoms leading to a sort of relaxation of locally constrained structures.

The time-averaged RMSF values, connected to

Table 1
Selected properties of AZ calculated from the MD simulated trajectories[a]

Parameter	Mean	S.D.	Min	Max	Drift
R_g (nm)	1.355	0.004	1.342	1.372	$< 10^{-6}$
E_{pot} (MJ/mol)	−185.33	0.49	−187.21	−183.16	−0.48
E_{kin} (MJ/mol)	31.73	0.24	30.84	32.71	−0.02
RMSD of all atoms (nm)	0.167	0.006	0.150	0.185	$1 \cdot 10^{-5}$
RMSD of C_α atoms (nm)	0.120	0.006	0.102	0.139	$5 \cdot 10^{-6}$

[a]All values are calculated during the 300–1100 ps time interval. S.D.: standard deviation; Min: minimal value; Max: maximal value; RMSD: root mean square deviations; R_g: radius of gyration; E_{pot}: total potential energy; E_{kin}: total kinetic energy. The drift values are calculated from a linear regression and are given per picosecond

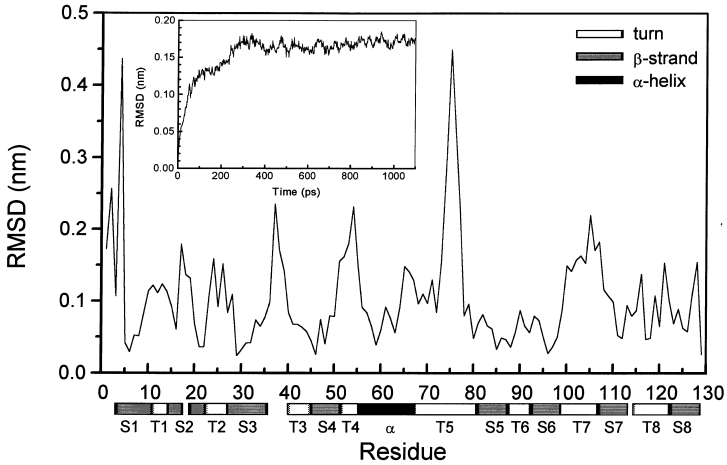

Fig. 2. The root mean square deviations (RMSD) between the crystallographic structure and the MD simulated conformation averaged over 300–1100 ps time interval plotted vs. backbone atoms (N, C_α, C, and O). Secondary structure elements are also shown. Inset: The RMSD of all atoms of AZ as a function of simulation time.

the extent of the protein motions during the simulation run, are shown as a function of the backbone atoms in Fig. 3. For comparison, the positional RMSF derived from crystallographic B-factors (broken line) are shown in the same figure. The two plots have similar trends and show main peaks at almost the same positions. The main differences are found in the T2, T3 and T8 turn regions and in the S6 β-strand. It should be considered that the values derived from crystallographic B-factors are indicative of atomic motion and conformational and lattice disorder, whereas the values calculated in the simulation are connected with almost internal motions of the protein itself [32].

Almost all the RMSF peaks observed in the simulated AZ protein are registered in correspondence of the turn regions. The largest values

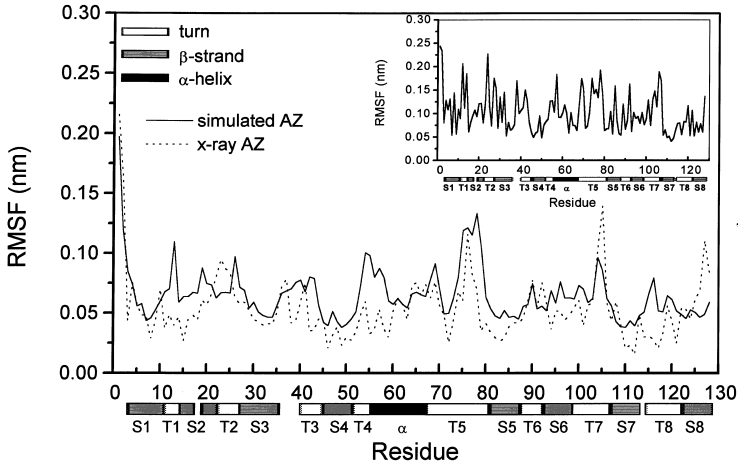

Fig. 3. Positional root mean square fluctuations (RMSF) of AZ plotted vs. backbone atoms (N, C_α, C, and O) calculated from the MD simulated structure averaged over a 300–1100-ps time interval (solid line) and obtained from crystal structure B factors (broken line). Inset: The RMSF of AZ plotted vs. side-chain atoms of protein residues calculated from the MD simulated structure averaged over a 300–1100-ps time interval. Secondary structure elements are also shown.

(> 0.10 nm) are observed for the 73–81 residues belonging to the T5 turn which connects the α-helix to the β-stranded core of AZ. Small fluctuations are, on the contrary, observed for residues forming the β-strands. Similar results have been found for PC [10], indicating that both the proteins show high mobility on the external surface, especially in turns and α-helix, and a rigid arrangement of the β-stranded protein skeleton. We observe also that the 36–44 residues, belonging to a random coil and to T3 turn, the 71–73 residues, which belong to T5 turn, the whole T6 and T8 turns, show low values of RMSF. These regions of protein could be particularly interesting since the T3, T5 and T6 turns are, in the folded protein, close to the copper site, and that the T8 turn contains His117 and Cys112, which are liganded to the copper ion, and most of the hydrophobic residues (114–117 and 119–120 residues), which play a crucial role in the electron transfer reaction with the physiological redox partners [17,18].

The RMSF of the side-chain atoms of the protein residues are shown in the inset of Fig. 3. These fluctuations are, on the average, larger than those registered for the backbone atoms, and their trend, as a function of the protein residues is similar to that seen for the backbone atoms; showing, indeed, the largest values (> 0.15 nm) in correspondence of almost all the turns and the lowest values in correspondence of residues forming β-strands, of 71–73 residues belonging to T5 turn and of the whole T8 turn. As already mentioned, the latter is rich in hydrophobic residues and also contains the His117 and Cys112 Cu-ligands. The overall higher RMSF values of side-chain atoms crudely indicate the accessibility of AZ atoms to solvent, which, in turn, may affect the mobility of specific regions of protein itself. The prevailing location of the side-chain atoms at the solvent accessible surface of the protein probably favours a large atomic mobility, while the motion of the backbone atoms is instead restrained by the rigid arrangement of the β-sandwich skeleton of the protein architecture. The overall emerging picture is that the protein regions, which are likely involved in the electron transfer process with reaction partners, are quite rigid and inaccessible to solvent, while all the turns and solvent accessible surface regions show high mobility.

Since the dynamics of intrinsic H-bonding network of protein is closely connected to the protein flexibility, the frequency of intraprotein H-bonds has been computed and compared with the crystallographic data [22]. A geometric criterion has been adopted to define the formation of an H-bond during the simulation was; namely, if the hydrogen to acceptor distance was shorter than 0.32 nm and the donor–acceptor angle was larger than 120° an H-bond was assumed to exist [33]. We have considered as maintained the H-bonds which are present in the simulation with a time percentage greater than 0.25; even if the donor or acceptor atom changes during the simulation.

Fig. 4 shows a diagram of the secondary structure elements, the H-bonds present in the crystallographic and/or in the simulated structure, the hydrophobic patch, the disulphide bridge and the copper ion. With regards to the backbone H-bonds, a comparison of our results with the crystallographic data reveals that 55 H-bond interactions are present also in the simulation; eleven are lost and nine new ones are formed. The H-bond network, involving backbone atoms, is particularly important to maintain and stabilize the secondary structure elements. Indeed, the close correspondence between the simulated and the crystallographic H-bond backbone network is particularly evident in the two β-sheets forming the AZ scaffold and in the α-helical region. In agreement with the β-sandwich structure description of AZ [22], no backbone H-bond is observed in the simulated structure among strands belonging to different sheets. A similar H-bonding pattern is also observed for PC [10]; revealing a similar dynamical evolution of the H-bonding interactions apt to maintain and stabilize the secondary structure of the two copper proteins. Rearrangements of the H-bond backbone network are observed in the T5 turn (from residues 68 to 80), namely two crystallographic H-bonds are lost (Lys70–Gly67 and Asp71–Lue68) and replaced by two new simulated ones (Lys70–Ser66, Asp71–Asp69). Moreover the two crystallographic H-bonds, Asp77–Lys74 and Val80–Asp77,

are definitively lost during the simulation conferring much higher mobility to the T5 turn connecting the α-helical structure element and the β-stranded core of protein. This mobility is indeed reflected in the high values observed for this turn in the RMSF data (see Fig. 3). In addition, three H-bond interactions, which are found only in the simulated structure, link S3 β-strand and T2 turn (Lys27–Lys24), α-helical region and S5 β-strand (Met56–Thr52), S8 β-strand and T8 turn (Lys122–Ser118). The losses and the new entries with respect to the crystallography could be due to the presence of hydration water, which partially competes with protein atoms to form H-bonds at the protein–solvent interface.

Fig. 4 shows also that a number of side-chains

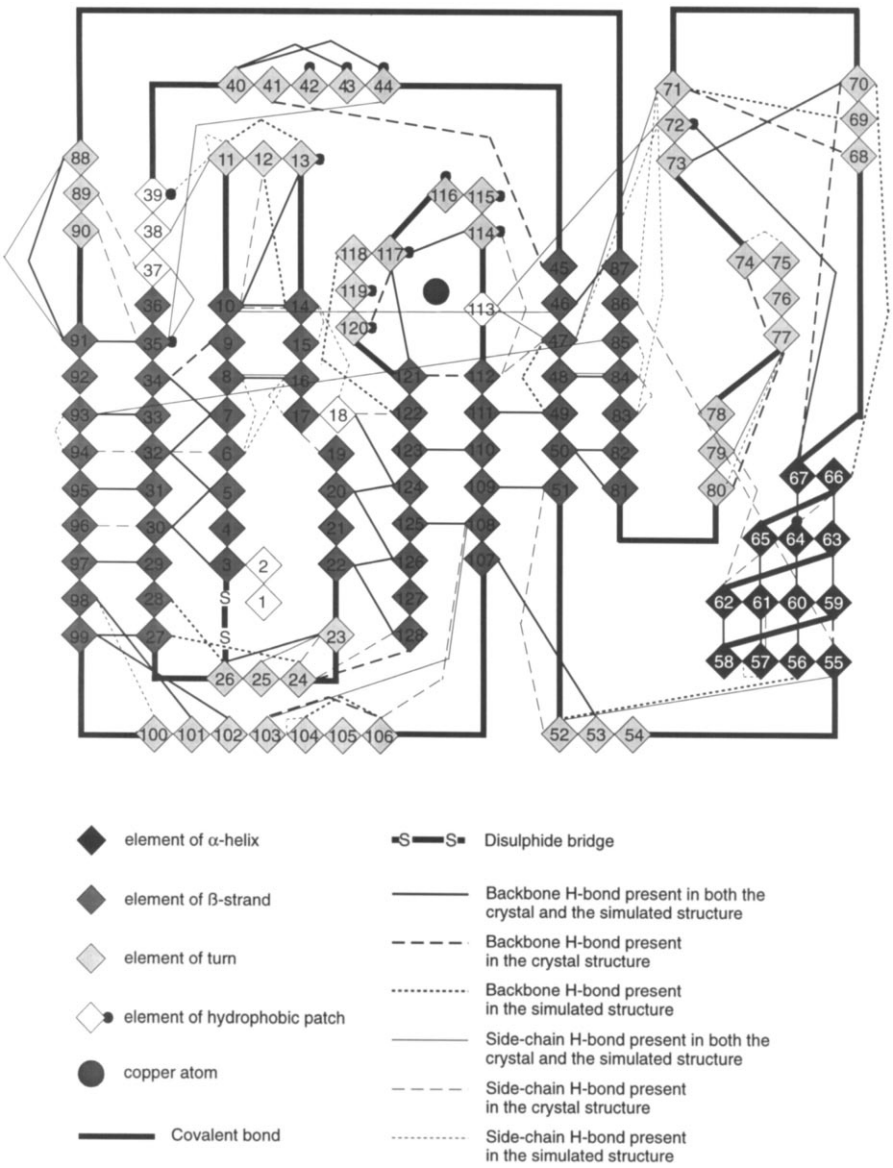

Fig. 4. Diagram of secondary structure elements of AZ with the crystallographic and simulated H-bonding pattern. Grey intensity represents secondary structure of aminoacids. The copper atom, the disulphide bridge and the hydrophobic patch are also indicated.

H-bonds are involved in stabilizing interactions in the tertiary structure of the protein. In particular in the simulated structure seventeen long-range interactions, in which a side-chain cross-links to a sequentially distant part of the polypeptide chain, are found. Only two of these H-bonds are found at the bottom, or southern end, of the molecule. One of them is present also in the crystallography (Tyr108–Lys103) and joins two parts of the same interstrand loop; the other one (Lys128–Lys24), which is found only in the simulated structure, joins the ends of two β-strands. On the contrary, most of the side-chains H-bonds, which are also present in the crystallography, are located at the northern end of the molecule, involving residues towards the ends of the β-strands and connecting turns at the top of the molecule. The overall emerging picture is that the southern end of the molecule, remote from the copper site, shows high mobility, while the structures surrounding the copper reaction center, at the northern end of the protein, show a rigid arrangement.

Besides a stabilization of the tertiary structure of the molecule, the H-bond interactions, which seem to confer rigidity at the copper site, may play an important role for the functionality of the protein. In this respect a recent hypothesis concerning the involvement of hydrogen bonds in the electron transfer mechanism has been suggested [2]. Indeed, there is, by now, considerable experimental evidences for electron transfer over long distances through saturated bonds whose electronic interactions decrease exponentially with the distance [21,34–36]. In AZ, which consists mainly in a highly interconnected β-sheet structure, the electron-transfer center is coupled strongly with the protein matrix [21]. In this respect, a through-bond tunneling model pathway, involving both polypeptide and hydrogen bonds, has been suggested to be related to the intramolecular electron transfer process from the disulphide bond, reduced in pulse radiolysis experiments, to the His46 Cu-ligand [19,20]. On such a basis, we remark that during the all simulation run the Asn10–His46 H-bond interaction is maintained; such an H-bond being supposed to play a crucial role in the intramolecular electron transfer process from the disulphide bond to the His46 Cu-ligand [19,20].

Generally, large-scale conformational transitions, which have been indicated as being relevant to the biological functions could be determined by relative and concerted movements between protein domains. In the electron transfer process, the motions of the protein atoms far from the copper site could facilitate a sequence of electron hops, or a large motion via superexchange, allowing the electron to travel a long distance from the docking site to the metal center [21].

On such a basis, we have analyzed the collective character exhibited by protein motions by means of DCCM. Cross-correlation coefficients range from a value of $+1$ for completely correlated motions to a value of -1 for completely anti-correlated motions. It should be, however, remarked that they do not bear any information about the magnitude of the motions; therefore, it may happen that both small- and large-scale collective motions were expressed by the same (C_{ij})[31]. Correlated interactions (with an absolute correlation coefficient value greater than 0.3) between different portions of the protein during an average simulation time of 700 ps are evident from the DCCM map shown in Fig. 5. Positive correlations (motions in the same direction) are plotted in the upper left triangle of the DCCM, while negative correlations (motions in opposite direction) are plotted in the lower right triangle. The plumes emanating from the diagonal are indicative of correlated motions between residues that are close in the primary structure and lie in the same secondary structure. Indeed, the plume emanating at and around (10,16) residues indicates time-correlated motions between S1 β-strand and S2 β-strand/T1 turn. Either isolated dots or clusters are present in the matrix. Most of the clusters are present in the upper left triangle. They represent positively correlated motions between pairs of adjacent β-strands. The ascending or descending trend is respectively correlated to the parallel or antiparallel coupling of strands in the folded protein structure. The presence of H-bonds connecting adjacent β-strands gives rise to correlated motions between the involved

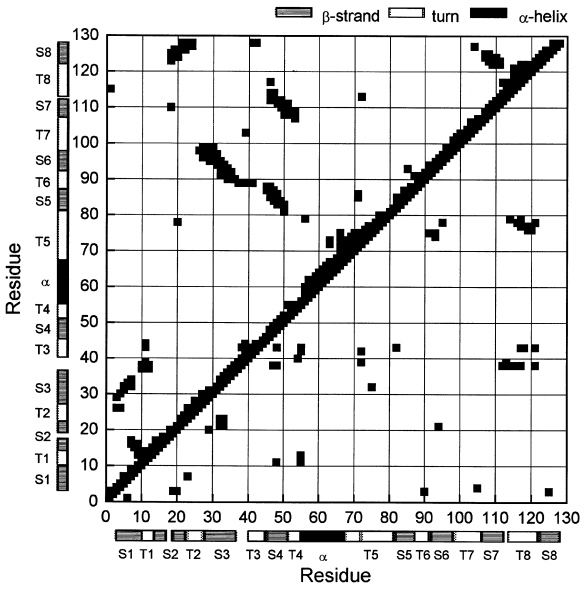

Fig. 5. Dynamical cross-correlation map (DCCM) for the C_α atom pairs of AZ averaged over a 300–1100-ps time interval. Only correlation coefficients with an absolute threshold value greater than 0.3 are shown. Positive correlations are mapped in the upper left triangle, negative correlations in the lower right triangle. Secondary structure elements are also shown.

residues; in this way, cross-correlation data provides information on the hydrogen bonding pattern allowing concerted motions without the breakdown of the protein secondary structure. We observe also a positive correlated cluster around (11,38) residues which lie close in the folded protein; it represents concerted motions between small 'domains' involving hydrophobic residues surrounding the copper ion. Again, a number of H-bonds are observed between these regions suggesting that a possible peculiar H-bonding pattern controls the motions of the protein important to the electron transfer process.

Of particular interest are the negative interactions shown in the lower right triangle of DCCM. Negative correlations occur mostly among residues that are far apart in the tertiary structure of the protein, with the only exception of two clusters involving residues (41,47) belonging to T3 turn and S4 β-strand and residues (74,91) belonging to T5 turn and S6 β-strand, which are close in space. Most of the negative clusters are indicative of anti-correlated motions between those turn regions which are putatively implied in the electron transfer process. Indeed, the clusters around (38,115), (43,117) and (76,116) residues are indicative of negative interactions of the coil region, T3 and T5 turns with the T8 turn, where the latter represent that region of protein mostly rich in hydrophobic residues and Cu-ligands. Other negative clusters are present in the map. In particular, the clusters around (12,53) and (40,53) residues represent anti-correlated interactions of the T1 and T3 turns, which are close to the copper site with the T4 turn, that is instead far from the metal reaction center. Such a behaviour suggests that small protein regions, remote from the copper site, move in a concerted way with far protein portions, which are close to the copper reaction center. In this respect, experimental and simulated studies on PC system suggested that the specific protein motions coupled to the electron transfer involve also directional correlated motions of atoms far from the copper site [26,37].

4. Conclusion

The analysis of some simulated parameters of fully hydrated AZ, such as the R_g, the total potential and kinetic energies, and RMSD has shown that during all the simulation run the protein maintains its globular shape and is almost stable. A detailed analysis of the RMSD and RMSF and of intraprotein H-bonding pattern has revealed that a rigid arrangement of the β-stranded protein skeleton is maintained during the simulation run, while large mobility is registered for the solvent-exposed regions, which are mostly influenced by water dynamics. In particular, such an influence is witnessed by the analysis of RMSD from the starting structure, which has mainly revealed that the residues located on the external surface show high values. The analysis of the intraprotein H-bonding network has pointed out a stabilization of the folded structure and a marked stiffness of the metal reaction center; the relevance of the latter feature being to be considered in the framework of the current through-bond tunneling model for the electron transfer process [21,34–36]. In this connection it could be

hypothesized that the H-bond network, subjected to continuous restructuring and solvent modulated dynamics, may provide a sort of preferentially route for the electron transfer in AZ. The analysis of the DCCM has indicated the presence of concerted motions among the residues that form the β-stranded scaffold surrounding the hydrophobic core and where the metal reaction center is situated. In addition, correlated and anti-correlated motions among protein regions, which are supposed to be involved in the electron transfer mechanism, have been observed and tentatively related to their possible role in the electron transfer process, where directional correlated motions of atoms far from the copper site could be involved [26,37].

The overall dynamical picture of AZ is very similar to that of PC [10], whose structural and functional properties are similar to those of the AZ, and is consistent with a general stiffness of the most important functional regions. The hydrophobic patch and the copper site show low mobility, while several dynamical rearrangements in the H-bonding pattern as due to solvation effect are observed.

References

[1] T. Alber, S. Daopin, K. Wilson, J.A. Wozniak, S.P. Cook, B.W. Matthews, Nature 330 (1987) 41.
[2] H. Frauenfelder, F. Parak, R.D. Young, Annu. Rev. Biophys. Chem. 17 (1988) 451.
[3] H. Frauenfelder, P.J. Steinbach, R.D. Young, Chem. Scri. 29A (1989) 145.
[4] J.L. Green, J. Fan, C.A. Angell, J. Phys. Chem. 98 (1994) 13780.
[5] C.X. Wang, A.R. Bizzarri, Y.W. Xu, S. Cannistraro, Chem. Phys. 183 (1994) 155.
[6] A.R. Bizzarri, C.X. Wang, W.Z. Chen, S. Cannistraro, Chem. Phys. 201 (1995) 463.
[7] A.R. Bizzarri, S. Cannistraro, Phys. Rev. E 53 (1996) 3040.
[8] C. Rocchi, A.R. Bizzarri, S. Cannistraro, Chem. Phys. 214 (1997) 261.
[9] C. Arcangeli, A.R. Bizzarri, S. Cannistraro, Chem. Phys. Lett. 291 (1998) 7.
[10] A. Ciocchetti, A.R. Bizzarri, S. Cannistraro, Biophys. Chem. 69 (1997) 185.
[11] M.R. Redinbo, T.O. Yeates, S. Merchant, J. Bioenerg. Biomembr. 26 (1994) 49.
[12] A. Paciaroni, M.E. Stroppolo, C. Arcangeli, A.R. Bizzarri, A. Desideri, S. Cannistraro, submitted to Eur. Biophys. J. (1998).
[13] A. Paciaroni, A.R. Bizzarri, S. Cannistraro, submitted to J. Mol. Liq. (1998).
[14] B. Frick, D. Richter, Science 267 (1998) 1939.
[15] A. Paciaroni, A.R. Bizzarri, S. Cannistraro, Phys. Rev. E 57 (1998) 6277.
[16] A. Paciaroni, A.R. Bizzarri, S. Cannistraro, Physica B (1998) in press.
[17] O. Farver, Y. Blatt, I. Pecht, Biochemistry 21 (1982) 3553.
[18] M. van de Kamp, M.C. Silvestrini, M. Brunori, J.V. Beeumen, F.C. Hali, G.W. Canters, Eur. J. Biochem. 194 (1990) 109.
[19] O. Farver, L.K. Skov, M. van De Kamp, G.W. Canters, I. Pecht, Eur. J. Biochem. 210 (1992) 399.
[20] O. Farver, L.K. Skov, G. Gilardi, G. van Pouderoyen, G.W. Canters, S. Wherland, I. Pecht, Chem. Phys. 204 (1996) 271.
[21] D.N. Beratan, J.N. Betts, J.N. Onuchic, Science 252 (1991) 1285.
[22] H. Nar, A. Messerschmidt, R. Huber, M. van de Kamp, G.W. Canters, J. Mol. Biol. 218 (1991) 427.
[23] W.F. van Gunsteren, H.J.C. Berendsen, Groningen Molecular Simulation (GROMOS) Library Manual, Biomos, Groningen, 1987.
[24] A.E. Mark, S.P. Helden, P.E. Smith, L.H.M. Janssen, W.F. van Gunsteren, J. Am. Chem. Soc. 116 (1994) 6293.
[25] K. Ugurbil, R.S. Norton, A. Allehand, R. Bersohn, Biochemistry 16 (1977) 886–894.
[26] L.W. Ungar, N.F. Scherer, G.A. Voth, Biophys. J. 72 (1997) 5.
[27] H.J.C. Berendsen, J.R. Grigera, T.P. Straatsma, J. Phys. Chem. 91 (1987) 6269.
[28] H.J.C. Berendsen, J.P.M. Postma, W.F. van Gunsteren, A. Di Nola, J.R. Haak, J. Chem. Phys. 81 (1984) 3684.
[29] J.P. Ryckaert, G. Ciccotti, H.J.C. Berendsen, J. Comput. Phys. 23 (1977) 327.
[30] R.M. Brunne, K.D. Berndt, P. Guntert, K. Wuthrich, W.F. van Gunsteren, Proteins: Struct., Funct. Genet. 23 (1995) 49.
[31] P.H. Hünenberger, A.E. Mark, W.F. van Gunsteren, J. Mol. Biol. 252 (1995) 492.
[32] G.A. Petsko, D. Ringe, Annu. Rev. Biophys. Bioeng. 13 (1984) 331.
[33] A.E. Garcia, L. Stiller, J. Comp. Chem. 14 (1993) 1396.
[34] O. Farver, I. Pecht, J. Am. Chem. Soc. 114 (1992) 5764.
[35] A. Broo, S. Larsson, Chem. Phys. 148 (1990) 103.
[36] J.N. Onuchic, D.N. Beratan, J.R. Winkler, H.B. Gray, Annu. Rev. Biophys. Biomol. Struct. 21 (1992) 349.
[37] E. Fraga, M.A. Webb, G.R. Loppnow, J. Phys. Chem. 100 (1996) 3278.
[38] P.J. Kraulis, J. Appl. Crystallogr. 24 (1991) 946.